Eur. Phys. J. D **39**, 129–140 (2006)
DOI: 10.1140/epjd/e2006-00081-7

THE EUROPEAN PHYSICAL JOURNAL D

Retrodiction for coherent communication with homodyne or heterodyne detection

O. Jedrkiewicz[1,a], R. Loudon[2], and J. Jeffers[3]

[1] INFM-CNR and Dipartimento di Fisica e Matematica, Universita' dell'Insubria, Via Valleggio 11, 22100 Como, Italy
[2] Department of Electronic Systems Engineering, University of Essex, Wivenhoe Park, Colchester CO4 3SQ, UK
[3] Department of Physics, University of Strathclyde, John Anderson Building, 107 Rottenrow, Glasgow G4 0NG, UK

Received 14 December 2005/ Received in final form 15 February 2006
Published online 11 April 2006 –

Abstract. Previous work on the retrodictive theory of direct detection is extended to cover the homodyne detection of coherent optical signal states $|\alpha\rangle$ and $|-\alpha\rangle$. The retrodictive input state probabilities are obtained by the application of Bayes' theorem to the corresponding predictive distributions, based on the probability operator measure (POM) elements for the homodyne process. Results are derived for the retrodictive information on the complex amplitude of the signal field obtainable from the difference photocount statistics of both 4-port and 8-port balanced homodyne detection schemes. The local oscillator is usually assumed much stronger than the signal but the case of equal strengths in 4-port detection is also considered. The calculated probability distributions and error rates are illustrated numerically for values of signal and local oscillator strengths that extend from the classical to the quantum regimes.

PACS. 42.50.-p Quantum optics – 42.50.Dv Nonclassical states of the electromagnetic field, including entangled photon states; quantum state engineering and measurements – 03.67.Hk Quantum communication

QICS. 01.10.+i Encoding, processing and transmission of information via physical systems

1 Introduction

The last fifty years have been characterised by rapid technological developments in the field of digital communications and digital data processing. Light-wave communication is now the preferred technology in many applications, and it relies on the success of optical fibre networks [1]. Although today's information systems operate within the domain of classical physics, quantum-mechanical signals can also be processed and transported. The properties of quantum systems can also be exploited in quantum cryptography to provide secure communications in optical fibre systems [2]. The essence of the communication problem is to determine the transmitted message from a knowledge only of the received signal. For this purpose the rigorous retrodictive formalism of quantum mechanics, where a state is assigned on the basis of the outcome of the measurement, can be adopted [3–6].

In optical communications, signals are constituted by a sequence of single bits of information, denoted by 0 or 1. Conventional optical communication systems operate in the classical multi-photon regime, where a received "1" may be represented by optical pulses containing for example about 10000 photons [2]. Coherent optical communications systems may use field modulation (amplitude, phase or frequency) instead of intensity modulation [1]. They employ highly coherent sources to produce binary signal pulses that can be represented, for example, by two coherent states with different well-defined phases as $|\alpha\rangle$ and $|-\alpha\rangle$. It is possible to measure the complex amplitude of the signal optical field by optical homodyne or heterodyne detection. In particular, homodyne detection is a fundamental method for the measurement of phase-sensitive properties of light [7–10]. In conventional four-port homodyne detection the local oscillator is prepared in an intense coherent state, so that the beam-splitter output coherent states are large in amplitude and approximately equal in intensity, allowing for their detection as photocurrents. In a balanced homodyne-detection scheme (using a 50:50 beam splitter) the quantum properties of the input field can be extracted from the difference photocount probability distribution [11–13]. Homodyne measurement techniques in the quantum regime with small amplitude (quantum-mechanical) coherent states, have also been investigated [12,13]; they have been applied for measuring statistical properties of the phase difference of two weak coherent fields [14,15]. Note that weak coherent fields are also used in some quantum cryptographic interference schemes, based (similarly to homodyne detection) on the coupling of two signals at a beam-splitter [2,16,17].

[a] e-mail: ottavia.jedrkiewicz@uninsubria.it

In this paper we extend our previous work on direct detection [6] to develop the predictive quantum-mechanical description of a coherent field measured by means of homodyne detection techniques, with the derivation of the probability operator measure (POM) elements describing the measurement process. Then with the retrodictive method derived from Bayes' theorem we calculate, given the result of the measurement, the input state probabilities for the information bits of a communication system described by the coherent field states $|\alpha\rangle$ or $|-\alpha\rangle$ only. The aim of these calculations is to apply a simple and direct procedure for deriving information about the nature of the binary signal sent into the communication channel. Thus, as in [6], we do not use the pure quantum-mechanical retrodictive formalism, but we rather use retrodiction as a calculational tool for the evaluation of the signal input state probabilities.

In Section 2, we consider four-port homodyne detection in detail and we derive the probability distributions for measurements of the photocount difference between the two output arms of the beam-splitter. Two interpretations for the quantum-mechanical descriptions of the signal evolution and detection process are given in Section 2.1. The output distributions corresponding to the measurement of the binary signal, together with the bit error rate in reception are shown in Section 2.2. We also calculate the retrodictive conditional probabilities associated with the input field states for conventional homodyne detection, and the probability of error occurring in the retrodiction process. Numerical results extending from the classical to the quantum regime are presented. The quantum-mechanical measurement of a coherent signal state in eight-port homodyne detection is treated in detail in Section 3, where the principal aim is to show how to derive the correct POM elements associated with the measurement outcomes. Two different approaches for this are considered in Sections 3.2 and 3.3 respectively. The input state retrodictive probabilities are given at the end of Section 3.3, and some comments on the similarity between the eight-port homodyne detection and the heterodyne detection schemes are presented. In Section 4, we present our conclusions.

2 Four-port homodyne detection

We consider a typical balanced four-port homodyne-detection scheme as shown in Figure 1. The signal field (operator $\hat{a}_s$) and the local oscillator field ($\hat{b}_l$), assumed to have the same frequency, are superimposed by a beam-splitter; the superimposed light in the two output channels (described by the operators $\hat{a}_{out}$ and $\hat{b}_{out}$) is recorded by two photodetectors (D_1 and D_2), and a correlator is used to derive the difference statistics of the recorded events. For a symmetric beam-splitter, the output field operators can be written as

$$\hat{a}_{out} = \frac{1}{\sqrt{2}}\left(\hat{a}_s + i\hat{b}_l\right), \quad \hat{b}_{out} = \frac{1}{\sqrt{2}}\left(\hat{b}_l + i\hat{a}_s\right), \qquad (1)$$

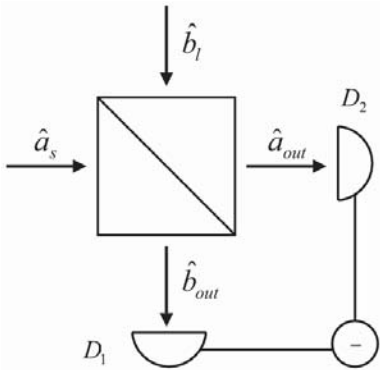

Fig. 1. Experimental scheme for balanced homodyne detection.

and in the ideal case of perfect detection, the operator for the photocount difference is simply

$$\hat{m}_{dif} \equiv \hat{m}_1 - \hat{m}_2 = \hat{b}^\dagger_{out}\hat{b}_{out} - \hat{a}^\dagger_{out}\hat{a}_{out} \rightarrow i\,|\beta|\left(\hat{a}_s \mathrm{e}^{-i\varphi_l} - \hat{a}^\dagger_s \mathrm{e}^{i\varphi_l}\right) = \hat{X}. \qquad (2)$$

In the last part of (2) $\hat{b}_l$ has been replaced by a c-number ($\hat{b}_l \rightarrow |\beta|\,\mathrm{e}^{i\varphi_l}$) assuming, as in conventional homodyne detection, the local oscillator to be very strong [13,18], and $\hat{X}$ denotes a quadrature operator for the signal field[1].

2.1 Output probability distributions and measurement POM elements

The photocount difference statistics can be derived from the joint photon-number probability distribution at the output of the beam-splitter. From the quantum theory of photodetection the latter is given by [13,19],

$$P_{m_1,m_2} = \left\langle : \frac{(\eta_1\hat{m}_1)^{m_1}}{m_1!}\mathrm{e}^{-\eta_1\hat{m}_1}\frac{(\eta_2\hat{m}_2)^{m_2}}{m_2!}\mathrm{e}^{-\eta_2\hat{m}_2} : \right\rangle, \qquad (3)$$

where m_1, m_2 are the counts recorded by the detectors D_1 and D_2 with quantum efficiencies η_1 and η_2 respectively. In general for an input coherent signal field $|\alpha\rangle$ with $\alpha = |\alpha|\,\mathrm{e}^{i\varphi_s}$, and a local coherent oscillator field $|\beta\rangle$ with $\beta = |\beta|\,\mathrm{e}^{i\varphi_l}$, equation (3) leads to

$$P_{m_1,m_2} = \frac{(\eta_1\theta_1/2)^{m_1}}{m_1!}\mathrm{e}^{-\eta_1\frac{\theta_1}{2}}\frac{(\eta_2\theta_2/2)^{m_2}}{m_2!}\mathrm{e}^{-\eta_2\frac{\theta_2}{2}}, \qquad (4)$$

where

$$\theta_{1,2} = |\alpha|^2 + |\beta|^2 \pm 2\,|\alpha|\,|\beta|\sin\left(\varphi_l - \varphi_s\right), \qquad (5)$$

the subscript "1" going with the "+" and the subscript "2" with the "–". In the following we consider $\eta_1 = \eta_2 = \eta$. The distribution of the difference events $m_{dif} = m_1 - m_2$ (<0 or >0) can be derived from (4) and can be written

[1] Note that the operator $\hat{X}$ introduced here is in fact proportional to the standard definition of quadrature operator that can be found in the literature (e.g. $i(\hat{a}\mathrm{e}^{-i\varphi} - \hat{a}^\dagger\mathrm{e}^{i\varphi})/2$), since strictly the signal field is independent of $|\beta|$.

to good approximation in the limit $|\beta|^2 \gg |\alpha|^2$ (which we assume from now on), as [13]:

$$P_{hom}^{pred}(m_{dif}) \cong \frac{1}{\sqrt{2\pi\eta\,|\beta|^2}} \times \exp\left[-\frac{[m_{dif} - 2\eta\,|\alpha|\,|\beta|\sin(\varphi_l - \varphi_s)]^2}{2\eta\,|\beta|^2}\right]. \quad (6)$$

The mean and the variance of the photocount difference distribution can be straightforwardly derived as

$$\begin{aligned}\langle m_{dif}\rangle &= i\langle\beta|\langle\alpha|\hat{b}_l^\dagger\hat{a}_s - \hat{a}_s^\dagger\hat{b}_l|\alpha\rangle|\beta\rangle \\ &= 2\eta|\alpha||\beta|\sin(\varphi_l - \varphi_s), \end{aligned} \quad (7)$$

and

$$\begin{aligned}(\Delta m_{dif})^2 &= -\langle\beta|\langle\alpha|(\hat{b}_l^\dagger\hat{a}_s - \hat{a}_s^\dagger\hat{b}_l)^2|\alpha\rangle|\beta\rangle \\ &\quad + (\langle\beta|\langle\alpha|\hat{b}_l^\dagger\hat{a}_s - \hat{a}_s^\dagger\hat{b}_l|\alpha\rangle|\beta\rangle)^2 \\ &= \eta^2(|\alpha|^2 + |\beta|^2) \cong \eta^2|\beta|^2. \end{aligned} \quad (8)$$

From now on we will mainly consider $\eta = 1$, with some comments on the case of imperfect detection in the discussions of Sections 2.2.1 and 2.2.2. In the predictive formalism $P_{hom}^{pred}(m_{dif})$ represents the conditional probability of recording m_{dif} difference photocounts, when the coherent state $|\alpha\rangle$ is sent into the homodyne detector. We also denote this probability by $P_{hom}^{pred}(m_{dif}\,|\alpha\,)$. Saying that the result of the measurement gives a number m_{dif} of counts, is equivalent to considering the measurement procedure formally described by the following POM element

$$\hat{\Pi}_{m_{dif}} = |m_{dif}\rangle\langle m_{dif}|. \quad (9)$$

The measurement is treated as a simple von Neumann measurement giving the eigenvalues of the photon-number difference operator $\hat{m}_{dif}$, and where the POM elements are thus projectors in the photon-number difference states basis. In the quantum-mechanical formalism, $P_{hom}^{pred}(m_{dif}\,|\alpha\,)$ can be written as [5]

$$P_{hom}^{pred}(m_{dif}\,|\alpha\,) = \mathrm{Tr}_{ls}\left[\hat{U}_{hom}\hat{\rho}_s \otimes \hat{\rho}_l\hat{U}_{hom}^\dagger\hat{\Pi}_{m_{dif}}\right], \quad (10)$$

where the density operators are $\hat{\rho}_s = |\alpha\rangle\langle\alpha|$, and $\hat{\rho}_l = |\beta\rangle\langle\beta|$. The unitary evolution operator denoted by $\hat{U}_{hom}$ describes the interaction of the signal field with the local oscillator field at the beam-splitter. The effect of the measurement procedure on the signal field, involving the interaction of the latter with the coherent oscillator field, is absorbed into the evolution process of the signal and thus into the evolution of the operator $\hat{\rho}_s$. In this picture, the effective measurement device could be represented by an abstract photodetector recording the number of difference counts.

An alternative description of the coherent state measurement performed with the four-port homodyne technique can be used. We can look at expression (6) as the probability distribution for the quadrature field operator in (2). The quadrature operator $\hat{X}$ depends on the local oscillator field amplitude and phase. The eigenstates $|X\rangle$ of $\hat{X}$ form a complete set of states and we can introduce, in analogy with (9), the following POM element

$$\hat{\Pi}_X = |X\rangle\langle X|. \quad (11)$$

We thus implicitly describe the measurement process using this POM element that contains the whole effect of homodyne detection. In other words, with respect to equation (9), here the information about the interaction between the local oscillator field and the coherent signal field is directly reflected in equation (11). The measured quantity is now the quadrature operator (2), and for a correct derivation of the corresponding probability distribution at the output of the homodyne-detection apparatus, we simply assume that there is no evolution of the signal field before the measurement. In this case, when we say "homodyne-detection apparatus", we imagine that the system represented by the beam-splitter, the local oscillator field entering from one of the two input channels, the two detectors and the correlator, constitute the measurement device as a whole, into which the signal field is simply fed.

In analogy with equation (10), the predictive conditional probability of measuring X (eigenvalue of the operator $\hat{X}$) for an input state $|\alpha\rangle$, is now

$$P_{hom}^{pred}(X\,|\alpha\,) = \mathrm{Tr}_s\left[\hat{\rho}_s\hat{\Pi}_X\right], \quad (12)$$

where $\hat{\Pi}_X$ is given by equation (11). Comparison of equation (12) with equation (10) shows that equation (11) can be rewritten as

$$\hat{\Pi}_X = \mathrm{Tr}_l\left[\hat{\rho}_l\hat{U}_{hom}^\dagger\hat{\Pi}_{m_{dif}}\hat{U}_{hom}\right]. \quad (13)$$

Thus we also have $P_{hom}^{pred}(X\,|\alpha\,) = |\langle\alpha\,|\,X\rangle|^2$, where $\langle\alpha\,|\,X\rangle \equiv \psi_\alpha(X)$ is the X quadrature representation of the coherent state $|\alpha\rangle$ [20,21]. By using the expansion of $|\alpha\rangle$ in terms of photon number states (12) can be written as

$$P_{hom}^{pred}(X\,|\alpha\,) = \frac{1}{\sqrt{2\pi\,|\beta|^2}} \times \exp\left[-\frac{(X - 2\,|\alpha|\,|\beta|\sin(\varphi_l - \varphi_s))^2}{2\,|\beta|^2}\right], \quad (14)$$

in accordance with previous results [13,20,21], and it can also be obtained from (6) via the equivalence (2) between m_{dif} and X. The above expression is a Gaussian distribution in quadrature space, equivalent to (6) and characterised by mean $\langle X\rangle$ and variance $(\Delta X)^2$ equal to (7) and (8) respectively (with $\eta = 1$).

Finally we note that the quadrature state $|X\rangle$ is similar to a squeezed state with squeezing parameter $s \to \infty$. We recall that the single mode squeezed state $|\alpha_s, \zeta\rangle$, with

$\zeta = s\,\mathrm{e}^{i\vartheta}$, satisfies the eigenvalue equation [11,20,21]

$$\left(\hat{a}_s \cosh s + \hat{a}_s^\dagger \mathrm{e}^{i\vartheta} \sinh s\right) |\alpha_s, \zeta\rangle = \left(\alpha_s \cosh s + \alpha_s^* \mathrm{e}^{i\vartheta} \sinh s\right) |\alpha_s, \zeta\rangle , \quad (15)$$

where $|\alpha_s, \zeta\rangle$ can also be written in terms of the Glauber displacement operator

$$\hat{D}\left(\alpha_s\right) = \mathrm{e}^{\alpha_s \hat{a}_s^\dagger - \alpha_s^* \hat{a}_s} \quad (16)$$

and the single-mode squeeze operator, acting on the signal mode vacuum

$$\hat{S}^{(1)}\left(\zeta\right) = \mathrm{e}^{(-\zeta \hat{a}_s^{\dagger 2} + \zeta^* \hat{a}_s^2)/2}, \quad (17)$$

as [20]

$$|\alpha_s, \zeta\rangle = \hat{D}\left(\alpha_s\right) \hat{S}^{(1)}\left(\zeta\right) |0\rangle_s = \mathrm{e}^{\alpha_s \hat{a}_s^\dagger - \alpha_s^* \hat{a}_s} \mathrm{e}^{(-\zeta \hat{a}_s^{\dagger 2} + \zeta^* \hat{a}_s^2)/2} |0\rangle_s . \quad (18)$$

By rewriting (2) in the form

$$\hat{X} = i\,|\beta|\,\mathrm{e}^{-i\varphi_l} \left(\hat{a}_s - \hat{a}_s^\dagger \mathrm{e}^{2i\varphi_l}\right), \quad (19)$$

the measured quantity in the homodyne detection process can thus be represented, apart from the factor $i\,|\beta|\,\mathrm{e}^{-i\varphi_l}$ (which is known), by the operator $\hat{a}_s - \hat{a}_s^\dagger \mathrm{e}^{2i\varphi_l}$. We see that the latter turns out to be proportional to the squeezing operator acting on $|\alpha_s, \zeta\rangle$ in (15), when $s \to \infty$ and with $\vartheta = 2\varphi_l + \pi$. The measurement can therefore be represented by projection onto the infinitely squeezed coherent state characterised by a complex amplitude α_s and by a phase angle $2\varphi_l + \pi$ determined by the phase of the coherent local oscillator [7,9].

2.2 Prediction and retrodiction for conventional homodyne detection

We now consider the four-port homodyne detection process at the output of a perfect communication channel, through which a binary coherent signal is sent. If the input signal is phase modulated, the information bits "0" and "1" contained in a train of pulses can be formally represented, for example, by the coherent states $|\alpha\rangle$ and $|-\alpha\rangle$. We assume that these bits are sent with equal prior probability. Because of the dependence of the output probability distributions (6) or (14), on the sine of the phase difference $\Delta\varphi$ between the local oscillator field and the signal field, we can choose φ_s and φ_l such that

$$\Delta\varphi = \varphi_l - \varphi_s = \pi/2 \;\text{ or }\; \Delta\varphi = \varphi_l - \varphi_s = -\pi/2. \quad (20)$$

One example would be to take α real and $\beta = i\,|\beta|$ when the states $|\alpha\rangle$ and $|-\alpha\rangle$ produce these two values of $\Delta\varphi$. The probability distributions (6) and (14) are then symmetric and in principle distinguishable at reception.

For simplicity, the prediction and the retrodiction process applied to the system under study will be discussed in this section by using the output distribution for the difference of photocounts m_{dif}. We should nevertheless keep in mind the perfect equivalence between (6) and (14).

2.2.1 Prediction and bit error rate in reception

We assume that the receiver can record the difference events m_{dif}. In conventional homodyne detection the local oscillator is characterised by a mean photon-number $\langle n_l\rangle = |\beta|^2$ much larger than the mean number of photons of the signal bits, $\langle n_s\rangle = |\alpha|^2$. The information about the signal phase is contained in the features of the output probability distributions associated respectively with the bit "0" and the bit "1", and which can be straightforwardly derived from equation (6) by taking into account equations (20). It can be easily checked by using equations (7) and (8) that $\Delta m_{dif}/\langle m_{dif}\rangle$ is independent of $|\beta|$, reflecting thus into the fact that we have a very poor discrimination of the two Gaussian distributions when $|\alpha|^2 \ll 1$. This implies that this kind of homodyne detection scheme is not suitable when the optical signal is extremely weak.

The performance of a digital communication system is measured by the probability of error per bit in reception, also called bit error rate (BER). For an on-off intensity modulated signal at the input of the optical transmitting device, if P_1 is the probability of mistaking "1" for "0", and P_0 is the probability of mistaking "0" for "1", and if the two bits are equally likely to be transmitted, then the BER is given by [1,22,23]:

$$\mathrm{BER} = \frac{1}{2}(P_0 + P_1). \quad (21)$$

A standard BER for classical information systems is 10^{-9} [1,2,24]. By analogy, in the context of homodyne detection, we denote by P_1 the probability of mistaking the state $|-\alpha\rangle$ for $|\alpha\rangle$, and by P_0 the probability of mistaking $|\alpha\rangle$ for $|-\alpha\rangle$. Then, treating in first approximation m_{dif} as a continuous variable, we can write in general

$$P_0 = \int_{-\infty}^{0} P_{hom}^{pred}\left(m_{dif}\,|\alpha\right) \mathrm{d}m_{dif}$$

$$\text{and} \qquad P_1 = \int_{0}^{+\infty} P_{hom}^{pred}\left(m_{dif}\,|-\alpha\right) \mathrm{d}m_{dif}. \quad (22)$$

The photocount difference distributions are perfectly symmetric with respect to the axis $m_{dif} = 0$, so $P_0 = P_1$, and in the case of perfect detection [24],

$$\mathrm{BER} = P_0 = P_1 = \frac{1}{\sqrt{2\pi\,|\beta|^2}} \int_0^\infty \exp\left[-\frac{\left(m_{dif} + 2\,|\alpha|\,|\beta|\right)^2}{2\,|\beta|^2}\right] \mathrm{d}m_{dif} = \frac{1}{2}\mathrm{erfc}\left(\frac{2\,|\alpha|}{\sqrt{2}}\right). \quad (23)$$

Denoting by Err the maximum required value for the bit error rate in reception ($Err \ll 1$), we can impose

$$\mathrm{BER} = \frac{1}{2}\mathrm{erfc}\left(\frac{2\,|\alpha|}{\sqrt{2}}\right) \leq Err. \quad (24)$$

This condition is independent of the amplitude of the local oscillator field. If the phase-modulated signal must be received with a probability of error $Err = 10^{-9}$, we find for the minimum number of photons required in the coherent signal state, $\langle n_s \rangle_{min} = |\alpha|^2_{min} \cong 9$, in accordance with previous results [24]. It is easy to check that for $\eta \neq 1$, the equivalent of (24) is

$$\mathrm{BER} = \frac{1}{2}\mathrm{erfc}\left(\frac{2\sqrt{\eta}\,|\alpha|}{\sqrt{2}}\right) \leq Err, \tag{25}$$

leading, when $Err = 10^{-9}$, to $\langle n_s \rangle_{min} = |\alpha|^2_{min} \cong 9/\eta$. Therefore, for a given BER in reception, the lower the detectors quantum efficiency, the higher must be the number of photons in the input coherent state, this scaling linearly with $1/\eta$.

2.2.2 Retrodiction and probability of error

The outcome of the single measurement performed by the photodetectors and processed by the correlator for each information bit sent and coupled with the local oscillator at the beam-splitter, gives a certain value for m_{dif}. We can retrodictively deduce from this value the probability that the signal state $|\alpha\rangle$ (formally bit "0") or $|-\alpha\rangle$ (formally bit "1"), has been sent through the detection device. We consider that the mean number of photons $\langle n_s \rangle$ contained in the "0" or in the "1" bit pulse, the mean number of photons $\langle n_l \rangle$ of the local oscillator and the phase difference $\Delta\varphi$, are known. Assuming then that the two bits of information "0" and "1" have the same transmission probability, we can write from Bayes' theorem the normalised retrodictive conditional probabilities for this system, as

$$P^{retro}_{hom}(\pm\alpha\,|m_{dif}) = \frac{P^{pred}_{hom}(m_{dif}\,|\pm\alpha)}{P^{pred}_{hom}(m_{dif}\,|\alpha) + P^{pred}_{hom}(m_{dif}\,|-\alpha)}, \tag{26}$$

where $P^{pred}_{hom}(m_{dif}\,|\alpha)$ and $P^{pred}_{hom}(m_{dif}\,|-\alpha)$ are obtained from (6). The expressions (26) depend on the measurement events m_{dif}. If $m_{dif} = 0$ we have as expected,

$$P^{retro}_{hom}(\alpha\,|m_{dif}) = P^{retro}_{hom}(-\alpha\,|m_{dif}) = 1/2, \tag{27}$$

independently of the amplitudes of the signal and local oscillator fields. The retrodictive conditional probability (26) is plotted in Figure 2, as a function of m_{dif} and for different values of $|\alpha|^2$ and $|\beta|^2$.

The probability of error in retrodicting the signal states $|\alpha\rangle$ and $|-\alpha\rangle$ depends on the value of m_{dif}. It can be shown that the fact that the bit error rate in the retrodiction process depends on the outcome of the measurement is similar to the case of direct detection at the output of an amplifier (in that case for an intensity modulated signal) [25]. For the homodyne detection system analysed here, we can say that given a number of recorded difference counts $m_{dif} > 0$, the input signal is in principle more likely to be $|\alpha\rangle$. On the other hand if $m_{dif} < 0$, the input pulse is more likely to be $|-\alpha\rangle$. Therefore the probability of error

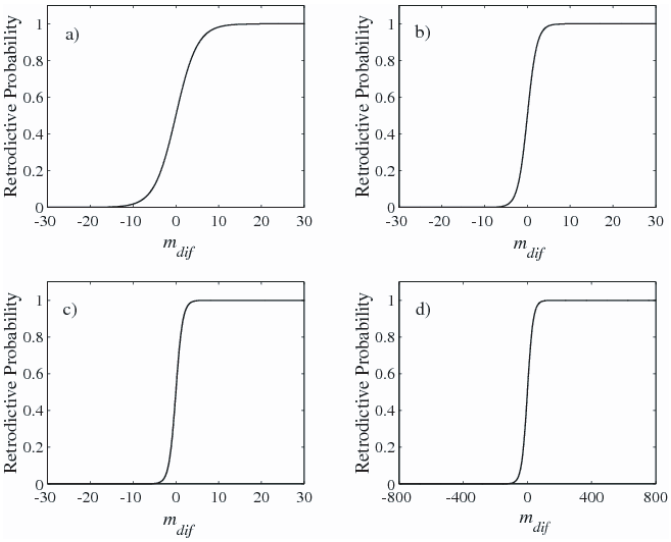

Fig. 2. Retrodictive conditional probability $P^{retro}_{hom}(\alpha\,|m_{dif})$ as a function of the measurement output m_{dif}, and for (a) $|\alpha|^2 = 1$, $|\beta|^2 = 100$, (b) $|\alpha|^2 = 5$, $|\beta|^2 = 100$, (c) $|\alpha|^2 = 10$, $|\beta|^2 = 100$, and (d) $|\alpha|^2 = 20$, $|\beta|^2 = 10^5$.

in retrodicting the state $|\alpha\rangle$ (situation where $\Delta\varphi = \pi/2$) can be represented by $P^{retro}_{hom}(-\alpha\,|m_{dif})$, while the probability of error in retrodicting the state $|-\alpha\rangle$ ($\Delta\varphi = -\pi/2$) can be represented by $P^{retro}_{hom}(\alpha\,|m_{dif})$.

If we need the BER in retrodiction to be smaller than a fixed quantity $Err \ll 1$, we can write when $m_{dif} > 0$, $P^{retro}_{hom}(-\alpha\,|m_{dif}) \leq Err$, and then from (26) and with the use of (6), we find

$$m_{dif}\frac{|\alpha|}{|\beta|} \geq \frac{1}{4}\ln\left(\frac{1-Err}{Err}\right). \tag{28}$$

Alternatively when $m_{dif} < 0$, imposing $P^{retro}_{hom}(\alpha\,|m_{dif}) \leq Err$, leads to the condition

$$m_{dif}\frac{|\alpha|}{|\beta|} \leq -\frac{1}{4}\ln\left(\frac{1-Err}{Err}\right). \tag{29}$$

It is worth noting here that equations (28) and (29) turn out to be *independent* of the detectors quantum efficiency, in contrast with (25). Moreover, contrary to (25), the expressions (28) and (29) depend on the ratio of the signal field amplitude to the local oscillator field amplitude; nevertheless they have been derived in the limit $|\beta|^2 \gg |\alpha|^2$. Similar to what can be found for direct detection in the amplifier case [25], there is here inevitably a range of values of m_{dif}, for which the probability of making a mistake when "deciding" which of the two bits of information constituted the signal is close to 1/2. Nevertheless we expect that the difference photocounts that do not satisfy equations (28) and (29) are associated with the overlap region between the left tail and the right tail of $P^{pred}_{hom}(m_{dif}\,|\alpha)$ and $P^{pred}_{hom}(m_{dif}\,|-\alpha)$ respectively. Thus they have a very small probability of being recorded. Error probabilities for retrodicting the signal states $|\alpha\rangle$ and $|-\alpha\rangle$, are plotted respectively at the top and bottom of Figure 3, in two

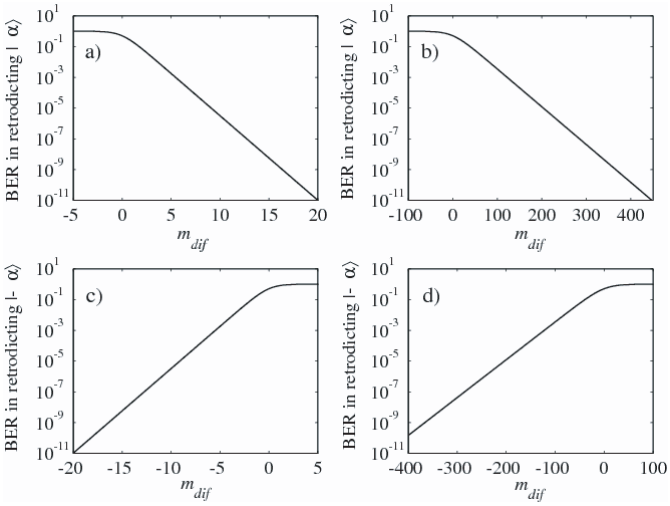

Fig. 3. Bit error rates in the retrodiction of the input states $|\alpha\rangle$ (top) and $|-\alpha\rangle$ (bottom) for $|\alpha|^2 = 10$ and $|\beta|^2 = 100$ (cases a, c), and for $|\alpha|^2 = 20$ and $|\beta|^2 = 10^5$ (cases b, d). The measurement is characterized by a mean value of difference counts respectively given by $\langle m_{dif}\rangle = 63$ (a), $\langle m_{dif}\rangle = 2828$ (b), $\langle m_{dif}\rangle = -63$ (c), and $\langle m_{dif}\rangle = -2828$ (d).

different cases. For values of m_{dif} falling around the mean value $\langle m_{dif}\rangle$, we find here a BER in retrodiction $\ll 10^{-15}$.

2.2.3 Prediction and retrodiction for equal amplitude signal and local oscillator fields

Huttner and coworkers have shown that an optimal error-free discrimination between two coherent states $|\alpha\rangle$ and $|-\alpha\rangle$ can be performed using a 50:50 beam-splitter to superpose the field mode known to be in one of these states with a mode prepared in the coherent state $|i\alpha\rangle$ [16,17]. This situation was considered in the context of quantum cryptography experiments based on the transmission of weak coherent states. By means of the formalism described above we can derive the difference statistics at the output of the four-port homodyne detector schematised in Figure 1 (also equivalent to the output of an interferometer as used in quantum cryptographic protocols), and the retrodictive probabilities for the input states, in the case where $|\alpha|^2 = |\beta|^2$. The theory applies for a general value of the amplitude $|\alpha|$. The signal information bits are represented by $|\alpha\rangle$ and $|-\alpha\rangle$ and are coupled at the beam-splitter to the local oscillator state $|i\alpha\rangle$. The expression for the joint probability distribution (4) can be used, leading, in the case of perfect detection to

$$P_{m_1,m_2} = \frac{(\theta_1/2)^{m_1}}{m_1!}\mathrm{e}^{-\frac{\theta_1}{2}}\frac{(\theta_2/2)^{m_2}}{m_2!}\mathrm{e}^{-\frac{\theta_2}{2}}, \qquad (30)$$

where now $\theta_{1,2} = 2|\alpha|^2 \pm 2|\alpha|^2 \sin\Delta\varphi$, and the two possible values for $\Delta\varphi$ are as in equation (20). If the input signal state is $|\pm\alpha\rangle$, we find from (30) $P_{hom}^{pred}(m_{dif} \geq 0\,|\alpha\rangle)$ (with $m_{dif} = m_1$) and $P_{hom}^{pred}(m_{dif} \leq 0\,|-\alpha\rangle)$ (with $m_{dif} = -m_2$) to be Poissonian distributions characterised by mean and variance given respectively by $\pm 2|\alpha|^2$ and $2|\alpha|^2$, in accordance with (7) and (8). Note that if the intensities of the optical signal and local oscillator are high, and thus $|\alpha|^2 \gg 1$, they are well approximated by Gaussian forms similar to (6) but with twice the variance $(=2|\alpha|^2)$.

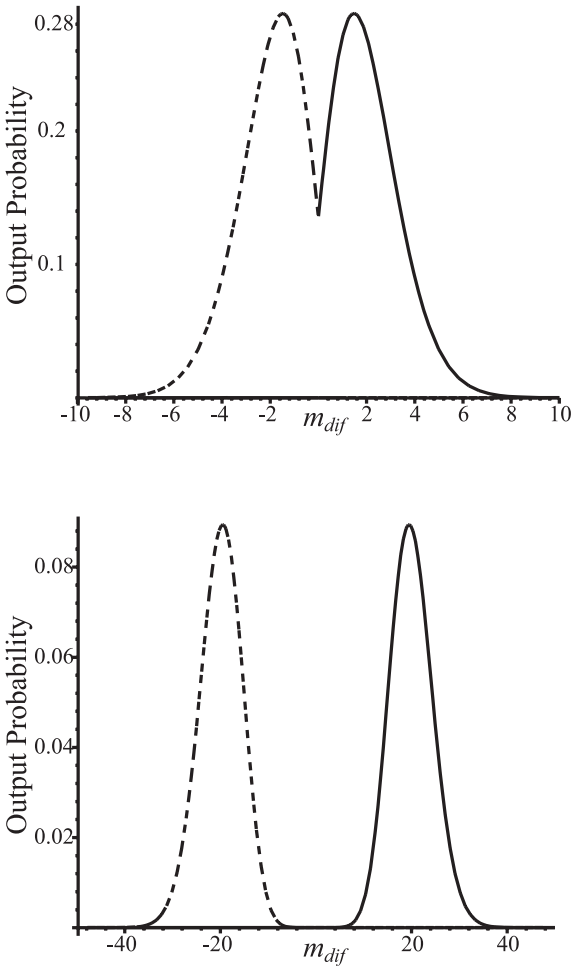

Fig. 4. Difference photocounts statistics corresponding to input signal states $|\alpha\rangle$ (full curve) and $|-\alpha\rangle$ (dashed curve), plotted for $|\alpha|^2 = |\beta|^2 = 1$ (top) and $|\alpha|^2 = |\beta|^2 = 10$ (bottom).

It can be easily shown using (1) that the interference process between the state $|\alpha\rangle$ or $|-\alpha\rangle$, and the state $|i\alpha\rangle$, transforms the input state $|\alpha\rangle_s|i\alpha\rangle_l$ or $|-\alpha\rangle_s|i\alpha\rangle_l$ into the output state $\left|i\sqrt{2\alpha}\right\rangle_1|0\rangle_2$ or $|0\rangle_1\left|-\sqrt{2}\alpha\right\rangle_2$, as previously noticed [16,17]. As a consequence, when photocounts are registered in one of the two (perfect) detectors, an unambiguous determination of the original state occurs at reception. The probability distributions $P_{hom}^{pred}(m_{dif} \geq 0\,|\alpha\rangle)$ and $P_{hom}^{pred}(m_{dif} \leq 0\,|-\alpha\rangle)$ are plotted in Figure 4 as functions of m_{dif} for $|\alpha|^2 = 1$ and $|\alpha|^2 = 10$. The two corresponding curves are in this case perfectly separated, in contrast to the case $|\beta|^2 \gg |\alpha|^2$, and they only overlap at $m_{dif} = 0$. The latter thus remains an uncertainty point for the discrimination between the two output distributions.

In this case the BER in reception is simply given by

$$\begin{aligned}\mathrm{BER} &= P_{hom}^{pred}\left(m_{dif}=0\,|\alpha\right)\\ &= P_{hom}^{pred}\left(m_{dif}=0\,|-\alpha\right)=\mathrm{e}^{-2|\alpha|^2}. \end{aligned} \tag{31}$$

This probability of error is very small in the limit $|\alpha|^2 \gg 1$. Note that the interference scheme discussed here could constitute a quantum cryptography experimental set-up [2,17], rather than being part of ordinary communication networks. In quantum cryptography, weak coherent signals are usually used for the quantum key distribution process, and measurements giving $m_{dif} = 0$ can be discarded. In that context, when $|\alpha|^2 \cong 0.1$ we have BER = 0.82, in accordance with the typical rate of discarded bits [2].

In the predictive approach, when input signal states $|\alpha\rangle$ or $|-\alpha\rangle$ are coupled at a 50:50 beam-splitter to a local oscillator described by $|i\alpha\rangle$, any outcome of the measurement that excludes the result $m_{dif} = 0$, gives a deterministic answer to the problem of knowing which of the two bit states $|\alpha\rangle$ or $|-\alpha\rangle$ constituted the optical signal. Calculation of the retrodictive input state preparation probabilities is thus straightforward. In fact using (26) we find, as expected,

$$P_{hom}^{retro}\left(\alpha\,|m_{dif}<0\right)=0,\;\; P_{hom}^{retro}\left(-\alpha\,|m_{dif}<0\right)=1, \tag{32}$$

$$P_{hom}^{retro}\left(\alpha\,|m_{dif}>0\right)=1,\;\; P_{hom}^{retro}\left(-\alpha\,|m_{dif}>0\right)=0, \tag{33}$$

and

$$P_{hom}^{retro}\left(\alpha\,|m_{dif}=0\right)=P_{hom}^{retro}\left(-\alpha\,|m_{dif}=0\right)=1/2. \tag{34}$$

At the end of Section 2.2.2 we have emphasised that, when $|\alpha|^2 \ll |\beta|^2$ and $|\alpha|^2 \ll 1$, the homodyne detection scheme illustrated is not suitable for a low-error discrimination process at the output, and as a consequence unsuitable for the uncertainty-free determination of which of the two states $|\alpha\rangle$ or $|-\alpha\rangle$ represented the optical signal, by retrodicting the result of the measurement. On the other hand, the contrasting case where $|\alpha|^2 = |\beta|^2$ can give, as shown here, good results for these purposes. Nevertheless if the amplitudes of the signal and local oscillator fields are very small, the probability of obtaining the (unwanted) measurement outcome $m_{dif} = 0$ is $\mathrm{e}^{-2|\alpha|^2} \approx 1 - 2\,|\alpha|^2$, thus very close to one. A system where $|\alpha|^2 = |\beta|^2 \gg 1$ then corresponds to the ideal situation for a correct determination of the input signal using retrodiction, with a low probability of error.

Finally in Figure 5, we have plotted the behaviours of $P_{hom}^{retro}\left(\alpha\,|m_{dif}\right)$ as a function of the coherent signal amplitude when $|\beta|^2 = 10^5$ and as a function of the local oscillator field amplitude when $|\alpha|^2 = 20$, and for two values of m_{dif} very close to the maximum uncertainty point $m_{dif} = 0$. We can see how $P_{hom}^{retro}\left(\alpha\,|m_{dif}\right) \to 1$ for $|\alpha|/|\beta| \to 1$.

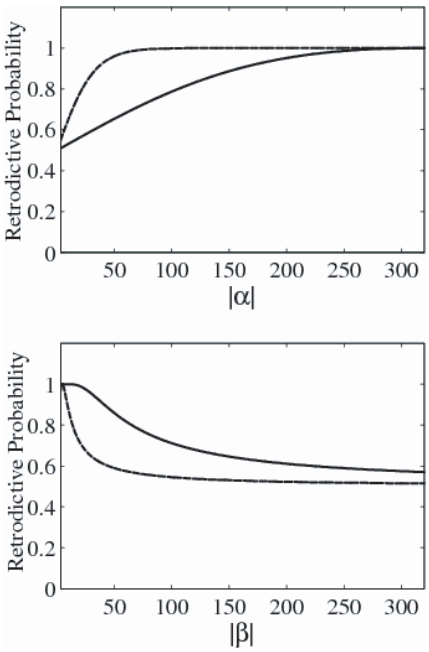

Fig. 5. $P_{hom}^{retro}\left(\alpha|m_{dif}\right)$ plotted respectively as a function of $|\alpha|$ for $|\beta|^2 = 10^5$ ($|\beta| \cong 316$) (top) and as a function of $|\beta|$ for $|\alpha|^2 = 20$ ($|\alpha| \cong 4.5$) (bottom). The full curves correspond to $m_{dif} = 1$ and the dashed curves correspond to $m_{dif} = 5$.

3 Eight-port homodyne detection (and heterodyne detection)

The principal aim of this section is to describe carefully the quantum-mechanical measurement of a coherent signal field for eight-port homodyne detection, and to derive the POM element associated with its outcome. The differences between this detection scheme and four-port homodyne measurements are pointed out. At the end of the section we give the expressions for the retrodictive conditional probabilities that can be calculated in order to obtain information on a binary phase-modulated coherent signal in optical communications. We also comment on the fact that the quantum-mechanical description of the measurement made here can also be applied to heterodyne detection.

3.1 The eight-port homodyne detection process

In Figure 6 a homodyne detector scheme characterised by four input ports and four output ports [10,11,26] is illustrated. Only two of the input ports are excited, one by the signal field and the other by the local oscillator field. The notations for the signal and local oscillator (or probe) fields annihilation operators are identical to those of Figure 1. The operators $\hat{a}_3$, $\hat{a}_4$ are associated with the unexcited input modes, and $\hat{d}_1$, $\hat{d}_2$, $\hat{d}_3$ and $\hat{d}_4$ characterise the output modes of the apparatus. In this case there are four detectors and although the correlators have not been schematised in the figure, the readings of the detectors

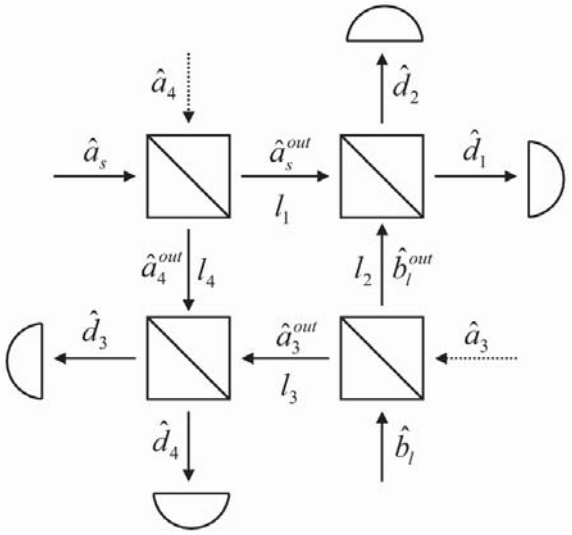

Fig. 6. Eight-port homodyne detector scheme.

are processed to provide the differences between the photocounts in adjacent pairs of output arms.

We assume that all the beam-splitters are 50:50 lossless beam-splitters. The field input–output relations at the top-left and bottom-right beam-splitters are respectively given by

$$\begin{cases} \hat{a}_s^{out} = \dfrac{1}{\sqrt{2}}\left(\hat{a}_s + i\hat{a}_4\right) \\ \hat{a}_4^{out} = \dfrac{1}{\sqrt{2}}\left(i\hat{a}_s + \hat{a}_4\right) \end{cases} \text{and} \quad \begin{cases} \hat{b}_l^{out} = \dfrac{1}{\sqrt{2}}(\hat{b}_l + i\hat{a}_3) \\ \hat{a}_3^{out} = \dfrac{1}{\sqrt{2}}(i\hat{b}_l + \hat{a}_3) \end{cases}. \tag{35}$$

Moreover at the output arms 1 and 2, and 3 and 4 respectively, we can write the following general relations

$$\text{and} \quad \begin{cases} \hat{d}_1 = \dfrac{1}{\sqrt{2}}\left(\hat{a}_s^{out} + ie^{i\varphi}\hat{b}_l^{out}\right) \\ \hat{d}_2 = \dfrac{1}{\sqrt{2}}\left(ie^{i\varphi}\hat{a}_s^{out} + \hat{b}_l^{out}\right) \end{cases} \quad \begin{cases} \hat{d}_3 = \dfrac{1}{\sqrt{2}}\left(e^{i\varphi'}\hat{a}_3^{out} + i\hat{a}_4^{out}\right) \\ \hat{d}_4 = \dfrac{1}{\sqrt{2}}\left(ie^{i\varphi'}\hat{a}_3^{out} + \hat{a}_4^{out}\right) \end{cases} \tag{36}$$

where φ and φ' are the phase shifts of the optical field associated with the path lengths difference $l_1 - l_2$ and $l_3 - l_4$ respectively. We choose the path lengths so that $\varphi = \pi/2$ and $\varphi' = \pi$, as usual in this kind of detection scheme [11]. We can now derive the operators for the photon-number differences between pairs of outputs, respectively denoted by $\hat{m}_{12}$ and $\hat{m}_{34}$. We assume that the detectors are perfectly efficient. Combining (36) with (35) and writing down only the terms that contribute to the expectation value of $\hat{m}_{12}$ and to its variance, we easily find

$$\hat{m}_{12} = \hat{d}_1^\dagger\hat{d}_1 - \hat{d}_2^\dagger\hat{d}_2 = \frac{1}{2}\left(\hat{a}_s^\dagger\hat{b}_l + \hat{b}_l^\dagger\hat{a}_s\right) + \frac{i}{2}\left(\hat{b}_l^\dagger\hat{a}_4 - \hat{a}_4^\dagger\hat{b}_l\right) + \frac{i}{2}\left(\hat{a}_s^\dagger\hat{a}_3 - \hat{a}_3^\dagger\hat{a}_s\right) + \ldots \tag{37}$$

and

$$\hat{m}_{34} = \hat{d}_3^\dagger\hat{d}_3 - \hat{d}_4^\dagger\hat{d}_4 = \frac{i}{2}\left(\hat{a}_s^\dagger\hat{b}_l - \hat{b}_l^\dagger\hat{a}_s\right) - \frac{1}{2}\left(\hat{b}_l^\dagger\hat{a}_4 + \hat{a}_4^\dagger\hat{b}_l\right) + \frac{1}{2}\left(\hat{a}_s^\dagger\hat{a}_3 + \hat{a}_3^\dagger\hat{a}_s\right) + \ldots \tag{38}$$

Note that the expectation values of the last two terms of (37) and of (38) are zero. These only contribute to the noise of the measured quantities. In Sections 3.2 and 3.3 we consider the case of conventional eight-port homodyne detection, and we thus assume that the local oscillator is a strong coherent field.

3.2 Two-quadrature field measurement and POM elements

If the intensity of the local oscillator is very strong, we can replace the annihilation operator $\hat{b}_l$ by the c-number $|\beta|\,e^{i\varphi_l}$, as done in (2). Equations (37) and (38) can then be rewritten as

$$\hat{m}_{12} \cong \frac{|\beta|}{2}\left[\left(\hat{a}_s + i\hat{a}_4\right)e^{-i\varphi_l} + \left(\hat{a}_s^\dagger - i\hat{a}_4^\dagger\right)e^{i\varphi_l}\right] \equiv \hat{X}_{12}, \tag{39}$$

and

$$\hat{m}_{34} \cong \frac{-i\,|\beta|}{2}\left[\left(\hat{a}_s - i\hat{a}_4\right)e^{-i\varphi_l} - \left(\hat{a}_s^\dagger + i\hat{a}_4^\dagger\right)e^{i\varphi_l}\right] \equiv \hat{Y}_{34}. \tag{40}$$

These are the operators describing the measured quantities, of which there are two, in contrast to four-port homodyne detection. The expression (39) represents the X quadrature of the operator $\hat{a}_s + i\hat{a}_4$, while (40) represents the Y quadrature of the operator $\hat{a}_s - i\hat{a}_4$, both characterised by phase $-\varphi_l$. Note that (39) and (40) are of the same form as (2) apart from the factor of 1/2. The operators $\hat{X}_{12}$ and $\hat{Y}_{34}$ satisfy the following commutation relation

$$\left[\hat{X}_{12}, \hat{Y}_{34}\right] = 0, \tag{41}$$

indicating that the two field quadratures (39) and (40) are independent quantum-mechanical variables, and thus that the quantities X_{12} and Y_{34} can be measured simultaneously. This occurs because of the inclusion, in the expressions for $\hat{m}_{12}$ and $\hat{m}_{34}$, of the terms in $\hat{a}_4$ and $\hat{a}_4^\dagger$; the commutator (41) does not vanish if these terms are neglected.

Similarly to the four-port homodyne detection, these independent measurements can be described in two ways: either they consist of recording the photon-number difference counts at the output of arms 1 and 2, and at the output of arms 3 and 4 respectively (after the signal field has interacted with the local oscillator field and with the vacuum field modes of the two unexcited input ports, inside the apparatus shown in Fig. 6); or alternatively the measurement processes can be seen as direct measurements of the quadratures (39) and (40) (by the "eight-port homodyne detector" interpreted as a whole and constituted by all the elements of Fig. 6). In this second picture there is

implicitly no evolution of the coherent signal before the measurement. From now on in this section we concentrate on the latter interpretation.

With the modes associated with the operators $\hat{a}_3$ and $\hat{a}_4$ in their vacuum states, the signal and the local oscillator in the coherent states $|\alpha\rangle$ and $|\beta\rangle$ respectively, and using (39) and (40), we find the expectation values of $\hat{X}_{12}$ and $\hat{Y}_{34}$ given by

$$\langle X_{12}\rangle = |\alpha|\,|\beta|\cos(\varphi_s-\varphi_l)\,,\ \langle Y_{34}\rangle = |\alpha|\,|\beta|\sin(\varphi_s-\varphi_l)\,, \tag{42}$$

and the variances by

$$(\Delta X_{12})^2 = \langle \hat{X}_{12}^2\rangle - \langle \hat{X}_{12}\rangle^2 \cong \frac{|\beta|^2}{2}$$
$$\text{and}\qquad (\Delta Y_{34})^2 = \langle \hat{Y}_{34}^2\rangle - \langle \hat{Y}_{34}\rangle^2 \cong \frac{|\beta|^2}{2}, \tag{43}$$

where terms of order $|\alpha|^2$ have been neglected. It is worth noting that if the quadrature operator (2) measured by the four-port detection apparatus were written in the same form as (39) or (40), and thus if it were multiplied by 1/2, the mean and the variance of (14) would be given by $|\alpha|\,|\beta|\sin(\varphi_l-\varphi_s)$ and $|\beta|^2/4$ respectively. Then here in the expressions for $(\Delta X_{12})^2$ and $(\Delta Y_{34})^2$, there is an extra contribution of $|\beta|^2/4$ coming from $\langle \hat{b}_l^\dagger \hat{a}_4 \hat{a}_4^\dagger \hat{b}_l\rangle/4$ and contained in $\langle \hat{X}_{12}^2\rangle$ and $\langle \hat{Y}_{34}^2\rangle$. This additional noise with respect to the four-port homodyne detection is due to the vacuum field in the unexcited input port at the top-left beam-splitter of Figure 6. In fact a similar noise contribution given by $|\alpha|^2/4$ (but which has been neglected in Eq. (43)) actually arises from a term of the form $\langle \hat{a}_s^\dagger \hat{a}_3 \hat{a}_3^\dagger \hat{a}_s\rangle/4$, when using (37) and (38), and is due to the presence of the vacuum field mode at the bottom-right beam-splitter of the same figure. In comparison to the four-port detector, the additional measurement capability of the eight-port detector is therefore gained at the expense of additional noise, in accordance with previous results [10,11].

Treating independently the measurements performed at the output arms 1 and 2, and at the output arms 3 and 4 respectively, and denoting by $|X_{12}\rangle$ and $|Y_{34}\rangle$ the eigenvalues of the quadrature operators $\hat{X}_{12}$ and $\hat{Y}_{34}$, we introduce the two corresponding POM elements as

$$\hat{\Pi}_{X_{12}} = |X_{12}\rangle\langle X_{12}| \quad\text{and}\quad \hat{\Pi}_{Y_{34}} = |Y_{34}\rangle\langle Y_{34}|\,, \tag{44}$$

similar to (11) and satisfying the required property of completeness [20]. The two normalised output probability distributions characteristic of eight-port homodyne detection are found to be respectively given by

$$P_{hom}^{pred}(X_{12}\,|\alpha\,) = \mathrm{Tr}_s\left[\hat{\rho}_s \hat{\Pi}_{X_{12}}\right]$$
$$= \frac{1}{\sqrt{\pi\,|\beta|^2}}\exp\left[-\frac{(X_{12}-|\alpha|\,|\beta|\cos(\varphi_s-\varphi_l))^2}{|\beta|^2}\right] \tag{45}$$

and

$$P_{hom}^{pred}(Y_{34}\,|\alpha\,) = \mathrm{Tr}_s\left[\hat{\rho}_s \hat{\Pi}_{Y_{34}}\right]$$
$$= \frac{1}{\sqrt{\pi\,|\beta|^2}}\exp\left[-\frac{(Y_{12}-|\alpha|\,|\beta|\sin(\varphi_s-\varphi_l))^2}{|\beta|^2}\right], \tag{46}$$

where we have set $\hat{\rho}_s = |\alpha\rangle\langle\alpha|$ as in Section 2. The means and variances of these Gaussian distributions are in accordance with (42) and (43).

Since in the limit of a strong local oscillator, the eight-port homodyne apparatus permits measurement of the two quantities (39) and (40), information on both the amplitude and phase of the coherent signal field can be extracted. In the following we show that this is the case, and we derive a single POM element describing the two-quadrature field measurement as a whole and the corresponding global output probability distribution, as an alternative to (44) and (45, 46). The formalism obtained can be straightforwardly applied to signal bits "0" and "1" sent through a communication channel and represented by the coherent states $|\alpha\rangle$ and $|-\alpha\rangle$, as described at the beginning of Section 2.2. The retrodictive conditional probabilities can then be directly calculated as will be shown at the end of the next section.

3.3 Coherent measurement POM and retrodiction

Using (39) and (40), we now introduce the linear combination

$$\hat{X}_{12} + i\hat{Y}_{34} = |\beta|\,\mathrm{e}^{-i\varphi_l}\left(\hat{a}_s + \hat{a}_4^\dagger \mathrm{e}^{i(2\varphi_l-\pi/2)}\right) \equiv |\beta|\,\mathrm{e}^{-i\varphi_l}\hat{A}, \tag{47}$$

where, as a consequence of the fact that $\hat{X}_{12}$ and $\hat{Y}_{34}$ are quantum-mechanically independent, $\hat{A}$ and $\hat{A}^\dagger$ commute

$$\left[\hat{A},\ \hat{A}^\dagger\right] = 0, \tag{48}$$

in contrast to the usual bosonic commutation relation. We can derive the POM element describing the abstract measurement of the observable $\hat{A}$, and we shall see that this turns out to be a coherent state projector. In order to work with quantities satisfying the canonical commutation relations characteristic of the field creation and annihilation operators, we introduce here, in analogy with equation (15), the two-mode squeezing operator [20]

$$\hat{A}_s = \hat{a}_s\cosh s + \hat{a}_4^\dagger \mathrm{e}^{i\vartheta}\sinh s, \tag{49}$$

where now $\vartheta = 2\varphi_l - \pi/2$. Note that in contrast to (48)

$$\left[\hat{A}_s,\ \hat{A}_s^\dagger\right] = \cosh^2 s - \sinh^2 s = 1. \tag{50}$$

The two-mode squeezed state $|\alpha_s, \alpha_4, \zeta\rangle$ satisfies the following eigenvalue relation [10,20]

$$\hat{A}_s\,|\alpha_s,\alpha_4,\zeta\rangle = \left(\alpha_s\cosh\ s + \alpha_4^* \mathrm{e}^{i\vartheta}\sinh\ s\right)|\alpha_s,\alpha_4,\zeta\rangle$$
$$\equiv A_s\,|\alpha_s,\alpha_4,\zeta\rangle\,, \tag{51}$$

with $\zeta = s\mathrm{e}^{i\vartheta}$, s being the squeezing parameter. It is seen from (47) and (48) that

$$\hat{A} = \lim_{s\to\infty} \frac{2}{\mathrm{e}^s}\hat{A}_s = \hat{a}_s + \hat{a}_4^\dagger \mathrm{e}^{i\vartheta}, \tag{52}$$

and the eight-port homodyne detection thus leads to a measurement associated with the state (51) in the limit of infinite squeezing. In order to show this, we start by considering the projector

$$\frac{\mathrm{e}^{2s}}{4}\left|\alpha_s, \alpha_4, \zeta\right\rangle\left\langle\alpha_s, \alpha_4, \zeta\right|. \tag{53}$$

This is a two-mode state projector, and since port 4 of Figure 6 is always in the vacuum, we can take the expectation value of (53) with respect to $|0\rangle_4$. Thus, using the fact that the state $|\alpha_s, \alpha_4, \zeta\rangle$ can be written in terms of Glauber operator defined in (16) and of the two-mode squeeze operator

$$\hat{S}^{(2)}(\zeta) = \mathrm{e}^{-\zeta \hat{a}_s^\dagger \hat{a}_4^\dagger + \zeta^* \hat{a}_s \hat{a}_4}, \tag{54}$$

and using the properties of the latter in accordance with (3.3.31) and (3.7.52) of [20] we evaluate the following projection

$$\begin{aligned} {}_4\langle 0|\alpha_s, \alpha_4, \zeta\rangle &= \hat{D}(\alpha_s)\ {}_4\langle 0|\hat{D}(\alpha_4)\hat{S}^{(2)}(\zeta)|0\rangle_s|0\rangle_4 \\ &= \hat{D}(\alpha_s)\ {}_4\langle 0|\mathrm{e}^{-\alpha_4^*\hat{a}_4 - \frac{1}{2}|\alpha_4|^2}\operatorname{sech} s \\ &\quad \times \sum_{n=0}^{\infty}\left[-\mathrm{e}^{i\vartheta}\tanh\, s\right]^n |n\rangle_s|n\rangle_4. \end{aligned} \tag{55}$$

The expression (55) can be simplified, leading to

$$\begin{aligned} {}_4\langle 0 \mid \alpha_s, \alpha_4, \zeta\rangle = \hat{D}(\alpha_s)\operatorname{sech} s\, \exp\Bigg[&-\frac{1}{2}|\alpha_4|^2 \\ &+ \frac{1}{2}|\alpha_4|^2 \tanh^2 s\Bigg] \left|\alpha_4^* \mathrm{e}^{i\vartheta}\tanh\, s\right\rangle_s \end{aligned} \tag{56}$$

where $\left|\alpha_4^* \mathrm{e}^{i\vartheta}\tanh s\right\rangle_s$ is a coherent state. For $s \to \infty$ (56) becomes

$$\begin{aligned} &{}_4\langle 0 \mid \alpha_s, \alpha_4, \zeta\rangle = \\ &2\mathrm{e}^{-s}\exp\left[\frac{1}{2}\left(\alpha_s\alpha_4 \mathrm{e}^{-i\vartheta} - \alpha_s^*\alpha_4^* \mathrm{e}^{i\vartheta}\right)\right]\left|\alpha_s + \alpha_4^* \mathrm{e}^{i\vartheta}\right\rangle_s. \end{aligned} \tag{57}$$

The prefactor of the coherent state on the right-hand side of (57) cancels when this expression is inserted into the projector defined in (53). The eight-port homodyne projector that describes the measurement performed by means of the apparatus of Figure 6 is thus a coherent-state projector of the form

$$\left|\alpha_s + \alpha_4^* \mathrm{e}^{i\vartheta}\right\rangle_s\ {}_s\left\langle\alpha_s + \alpha_4^* \mathrm{e}^{i\vartheta}\right| \equiv |\gamma\rangle\langle\gamma| \tag{58}$$

conveniently expressed in terms of shorthand γ. The normalized POM element can finally be defined as

$$\hat{\Pi}_\gamma = \frac{1}{\pi}|\gamma\rangle\langle\gamma|, \tag{59}$$

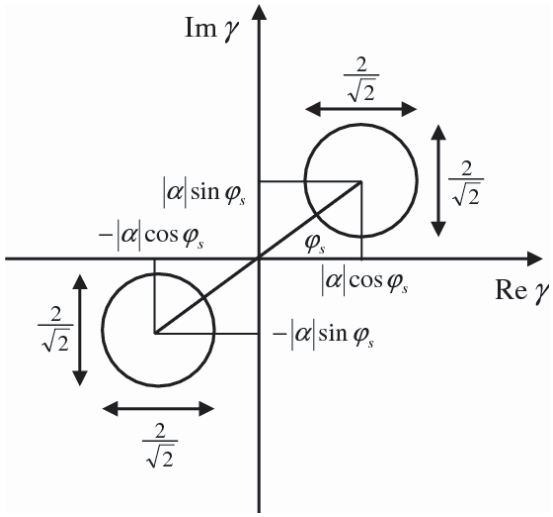

Fig. 7. Phase-space description of the mean values and uncertainties of the real and imaginary parts for the measured coherent state in eight-port homodyne detection. The circle in the first quadrant corresponds to an input signal state $|\alpha\rangle$, while the circle in the third quadrant corresponds to an input signal state $|-\alpha\rangle$.

in accordance with previous results [9], and satisfying the required normalisation condition [20].

For a measurement performed on a coherent signal $|\alpha\rangle$, the corresponding probability distribution is a phase-space distribution given by

$$P_{hom}^{pred}(\gamma\,|\alpha\,) = \mathrm{Tr}_s\left[\hat{\rho}_s\hat{\Pi}_\gamma\right] = \frac{1}{\pi}\mathrm{e}^{-|\gamma-\alpha|^2}, \tag{60}$$

with properties

$$\langle \mathrm{Re}\,\gamma\rangle = \mathrm{Re}\,\alpha = |\alpha|\cos\varphi_s, \quad \langle \mathrm{Im}\,\gamma\rangle = \mathrm{Im}\,\alpha = |\alpha|\sin\varphi_s, \tag{61}$$

$$(\Delta \mathrm{Re}\,\gamma)^2 = (\Delta \mathrm{Im}\,\gamma)^2 = \frac{1}{2}. \tag{62}$$

The real and imaginary parts of the coherent state γ are therefore independent Gaussian variables (this is a consequence of the commutation property (48) and thus also of Eq. (41)), with means given by the real and the imaginary parts of the signal field α, and common variance 1/2. Note that the latter is twice the coherent state quadrature value and, similar to that discussed in Section 3.2, the extra noise contribution (of 1/4) is due to the presence of the unexcited input port 4 of Figure 6. It is easy to show that equation (60) can be rewritten as

$$P_{hom}^{pred}(\gamma\,|\alpha\,) = P_{hom}^{pred}(\mathrm{Re}\,\gamma\,|\alpha\,)\,P_{hom}^{pred}(\mathrm{Im}\,\gamma\,|\alpha\,), \tag{63}$$

where $\mathrm{Re}\,\gamma = |\gamma|\cos\varphi_\gamma$ and $\mathrm{Im}\,\gamma = |\gamma|\sin\varphi_\gamma$. Here in contrast to four-port homodyne detection, the simultaneous measurement of the amplitude $|\gamma|$ and of the phase φ_γ then corresponds to the *simultaneous* noisy observation of the amplitude and the phase of the signal, $|\alpha|$ and φ_s. Figure 7 shows geometrical representations of the measured coherent state $|\gamma\rangle$, when the signal is given by $|\alpha\rangle$ and

$|-\alpha\rangle$ respectively. These representations also give some information about the projections (in the plane of the field quadratures) of the probability distributions $P_{hom}^{pred}(\gamma\,|\alpha\,)$ and $P_{hom}^{pred}(\gamma\,|-\alpha\,)$ respectively (the diameters of the circles representing here twice the square root of the variance associated with the measurement).

Experimentally the results of the two measurements performed at the top-right and bottom-left beam-splitters of Figure 6 can be therefore processed in order to give the value of the amplitude and phase of the measured quantity γ. In the case of a binary communication system, we can then associate with the measurement of the coherent bits of information "0" and "1" (represented by the states $|\alpha\rangle$ and $|-\alpha\rangle$), the probability distributions in the phase-space representation given by $P_{hom}^{pred}(\gamma\,|\alpha\,)$ and $P_{hom}^{pred}(\gamma\,|-\alpha\,)$ respectively. Interpreting the complex number γ as the final outcome of the detection event, and assuming that the two signal states have the same probability of occurrence, we can then derive the retrodictive conditional probabilities for these states, by using Bayes' theorem in the simple form

$$P_{hom}^{retro}(\pm\alpha\,|\gamma\,)=\frac{P_{hom}^{pred}(\gamma\,|\pm\alpha\,)}{P_{hom}^{pred}(\gamma\,|\alpha\,)+P_{hom}^{pred}(\gamma\,|-\alpha\,)}, \quad (64)$$

where $P_{hom}^{pred}(\gamma\,|\alpha\,)$ and $P_{hom}^{pred}(\gamma\,|-\alpha\,)$ are obtained as products of measured output distributions as shown in equation (63). Similarly to equation (26), these retrodictive probabilities associated with the input signal states depend on the overlap of the measured probability distributions; but in contrast to four-port homodyne detection, this overlap occurs in the phase-space representation and thus in two dimensions, as it appears in Figure 7. We thus expect that the more the distributions $P_{hom}^{pred}(\gamma\,|\alpha\,)$ and $P_{hom}^{pred}(\gamma\,|-\alpha\,)$ are distinguishable and therefore well separated, the better the retrodictive expressions (64) lead to a clear and deterministic result for deciding which of the two coherent states, $|\alpha\rangle$ or $|-\alpha\rangle$, constituted the signal. The additional noise in the eight-port detection scheme leads to the conclusion that four-port homodyne detection is more useful for discrimination of the states $|\alpha\rangle$ and $|-\alpha\rangle$ in coherent communications.

Finally we comment briefly on the similarity between the quantum-mechanical description of the eight-port homodyne detection process and the heterodyne detection process. In heterodyne detection the signal is mixed with a strong coherent local oscillator (probe) at a beam-splitter, as in the scheme of Figure 1, and the measurement usually consists in detecting the resulting field (photocurrent) at one of the two output ports (or in some cases at both ports) of the beam-splitter [27]. The difference with homodyne detection is that the frequencies of the local oscillator field and the signal field are not the same [18,27]. Three frequency modes eventually contribute to the detection process, these being the probe frequency ω_l, the signal field frequency ω_s, and the frequency $2\omega_l-\omega_s$ of the "image" mode. A filtering procedure is adopted where the field resulting from the superposition of the signal and the strong probe is mixed with a classical field, and then followed by the detection of the d.c. component. The data can be processed in such a way that both the quadratures of the signal field can be extracted and thus information on both the amplitude and phase of the coherent signal can be obtained, as in eight-port homodyne detection. In fact it can be shown that the heterodyne apparatus realises the abstract quantum measurement of an operator having the form $\hat{a}_s+\hat{a}_I^{\dagger}e^{i\phi}$, where $\hat{a}_I^{\dagger}$ is the creation operator associated with the image mode, which similarly to the mode of the input port 4 of Figure 6, is in the vacuum state. Because of the similarity of $\hat{a}_s+\hat{a}_I^{\dagger}e^{i\phi}$ to the operator $\hat{A}$ defined in equation (47), we can in fact describe this measurement process in an identical way to the one used here for eight-port homodyne detection, in agreement with previous work [10,27]. The POM element associated with the outcome of the abstract measurement in heterodyne detection can again be written as a coherent state projector, similar to equation (59), and the resulting output distribution gives information about both the amplitude and phase of the coherent signal state.

4 Conclusions

In this paper we have analysed the quantum-mechanical measurement process of a coherent signal state by means of four-port and eight-port homodyne detection techniques. In four-port homodyne detection the retrodictive process that can be used in order to derive information about the nature of the phase-modulated coherent signal, has been described in detail. Thus in Section 2 we have first analysed the predictive output probability distributions associated with the two signal bits "0" and "1" (represented by the coherent states $|\alpha\rangle$ and $|-\alpha\rangle$) with the bit error rate in reception. We then calculated and studied the retrodictive conditional probabilities of having the signal constituted by one of these two bits, given the outcome of the measurement, with the corresponding probabilities of error.

In balanced four-port detection, the outcome of the measurement is given by the photocount difference between the two output arms of the beam-splitter. We have seen in Section 2.1 that the difference counts statistics is also equivalent to the signal field quadrature probability distribution. The POM element associated with the measurement outcome has been correspondingly derived. This can be written as a difference count photon-number projector, when we assume that in the homodyne detection apparatus the coherent signal field first undergoes an evolution due to its interaction with the local oscillator field, and is then effectively measured. Alternatively considering that there is no evolution of the signal field between preparation and measurement, the measurement process and the effect of the whole homodyning procedure can be simply enclosed in a POM element written as a quadrature field projector.

The retrodictive conditional probabilities have then been derived, by using Bayes' theorem, in terms of the

output probability distributions describing the statistics of the difference of photocounts registered at the two output arms of the beam-splitter (in the case of perfect detection). In conventional homodyne detection, where the local oscillator field is assumed to be very much stronger than the signal, we have seen that in the particular case where the mean number of photons in the signal field is much smaller than one, the results are not really satisfactory, and retrodicting the input state probabilities does not give precise information on the nature of the signal. Optimal discrimination between the measured output distributions occurs when the amplitudes of the signal and local oscillator fields are the same. Consequently deterministic results in the retrodiction process can then be obtained, apart from when the recorded number of difference counts is zero.

In Section 3 we have provided a quantum-mechanical description of the measurement of a coherent state performed by means of the eight-port homodyne detection apparatus. In the limit of strong local oscillator we have seen in Section 3.2 that two field quadratures can be simultaneously measured, giving information on both the amplitude and the phase of the signal, although (with respect to the four-port detection) at the expense of additional noise in accordance with previous results [10,11]. In Section 3.3 we have presented a rigorous derivation of the POM element that is often used [9,27] to describe the effective abstract measurement resulting from the use of this eight-port homodyne apparatus, given by a coherent state projector. The retrodictive conditional probabilities for input coherent signal bits, described by $|\alpha\rangle$ or $|-\alpha\rangle$, have been found and briefly commented on at the end of the section, by using Bayes' theorem in conjunction with the measured output distributions of the system written in the phase-space representation. We have also pointed out the similarity between the eight-port homodyne and the heterodyne measurement processes.

The retrodictive approach, developed here for homodyne detection, has the same advantages as in its use for the study of optical information transfer by direct detection, considered previously [6]. Conventional theory takes the viewpoint of the transmitter of information, so it requires a determination of the behavior of input signals as they propagate through the system to the receiver. The corresponding calculations determine the distribution of received output signals generated by known input signals. However, in practice, the viewpoint of the recipient of information, who looks backwards through the system and needs to determine the distribution of transmitted input signals implied by known output signals, is of greater interest. Both kinds of analysis, predictive and retrodictive, are based on the same properties of the transmission system but the relations between the two are nontrivial. The calculations presented here provide the required results for the main varieties of phase-sensitive detection in coherent communications.

The authors would like to thank the UK Engineering and Physical Sciences Research Council for financial support.

References

1. B.E.A. Saleh, M.C. Teich, *Fundamentals of photonics* (John Wiley & Sons, 1991)
2. P.D. Townsend, Opt. Fiber Techn. **4**, 345 (1998), and see references therein.
3. S.M. Barnett, D.T. Pegg, Phys. Rev. A **60**, 4965 (1999)
4. S.M. Barnett, D.T. Pegg, J. Jeffers, J. Mod. Opt. **47**, 1779 (2000)
5. S.M. Barnett, D.T. Pegg, J. Jeffers, O. Jedrkiewicz, R. Loudon, Phys. Rev. A **62**, 022313 (2000)
6. O. Jedrkiewicz, R. Loudon, J. Jeffers, Phys. Rev. A **70**, 033805 (2004)
7. H.P. Yuen, J.H. Shapiro, IEEE Trans. Inf. Theory **24**, 657 (1978)
8. J.H. Shapiro, H.P. Yuen, J.A. Machado Mata, IEEE Trans. Inf. Theory **25**, 179 (1979)
9. H.P. Yuen, J.H. Shapiro, IEEE Trans. Inf. Theory **26**, 76 (1980)
10. N.G. Walker, J. Mod. Opt. **34**, 15 (1987)
11. R. Loudon, in *Frontiers in quantum optics*, edited by E.R. Pike, S. Sarkar (Adam Hilger, Bristol, 1986), p. 42
12. S.L. Braunstein, Phys. Rev. A **42**, 474 (1990)
13. W. Vogel, J. Grabow, Phys. Rev. A **47**, 4227 (1993)
14. J.W. Noh, A. Fougères, L. Mandel, Phys. Rev. Lett. **67**, 1426 (1991)
15. J.W. Noh, A. Fougères, L. Mandel, Phys. Rev. A **45**, 424 (1992); J.W. Noh, A. Fougères, L. Mandel, Phys. Rev. A **46**, 2840 (1992)
16. B. Huttner, N. Imoto, N. Gisin, T. Mor, Phys. Rev. A **51**, 1863 (1995)
17. S.M. Barnett, Phil. Trans. R. Soc. Lond. A **355**, 2279 (1997)
18. H. Fearn, R. Loudon, T.J. Shepherd, J. Opt. Soc. Am. B **8**, 2218 (1991)
19. R.J. Glauber, in *Quantum optics and electronics*, edited by C. De Witt, A. Blandin, C. Cohen-Tannoudji (Gordon and Breach, New York, 1965)
20. S.M. Barnett, P.M. Radmore, *Methods in theoretical quantum optics* (Clarendon Press, Oxford, 1997)
21. H.P. Yuen, Phys. Rev. A **13**, 2226 (1976)
22. T. Li, M.C. Teich, IEEE J. Quant. Electron. **29**, 2568 (1993)
23. M. Schwartz, *Information, transmission, modulation and noise* (McGraw-Hill Publishing Company, 1990)
24. Y. Yamamoto, Trans. IEICE **73**, 1598 (1990)
25. O. Jedrkiewicz, *Theories of atom-field interaction in cavities and retrodiction for quantum communications*, Ph.D. thesis, Chap. 8 (University of Essex, UK, 2001)
26. N.G. Walker, J.E. Carroll, Electron. Lett. **20**, 981 (1984)
27. J.H. Shapiro, S.S. Wagner, IEEE J. Quant. electron. QE **20**, 803 (1984)